JOURNAL OF SOLID STATE CHEMISTRY 79, 119–125 (1989)

Crystal Growth and Properties of $BaSn_2Fe_4O_{11}$

M. DROFENIK, D. HANŽEL, AND DARKO HANŽEL
"Jožef Stefan" Institute, Ljubljana 39, Yugoslavia

AND M. N. DESCHIZEAUX-CHÉRUY AND J. C. JOUBERT
Ecole Nationale Supérieure de Physique de Grenoble, France

Received June 8, 1988; in revised form November 15, 1988

Single crystals of $BaSn_2Fe_4O_{11}$ were grown from a BaO–B_2O_3 flux and examined using X-ray diffraction analyses and Mössbauer spectroscopy. It was found that the grain growth conditions influence the properties of these crystals. A higher soaking temperature changes the distribution of Sn and Fe on 4e and 6g lattice sites. © 1989 Academic Press, Inc.

Introduction

Magnetoplumbite and related ferrites form an extended group of magnetic oxides which exhibit marked magnetocrystalline anisotropy. This property is utilized in the ferrite permanent magnet material $BaFe_{12}O_{19}$ and in some microwave materials. Common to the whole group are "structural units" from which these compounds are built. For example, $BaFe_{12}O_{19}$ can be described as a stacking of two spinel blocks (S) and two R blocks and can be labeled as $(SR)_2$.

Recently a series of isostructural compounds $BaM_2Fe_4O_{11}$ where M (Ti, Sn, Mn, Ru, Cr) was composed of two R blocks, R_2, were reported (*1, 2*). In these compounds the R structural unit determines their structural and magnetic properties. Knowledge of structural and magnetic properties of such elementary structural blocks is important for better understanding of the whole group of compounds. The investigation of polycrystalline samples is in most cases of a qualitative nature. For more quantitative study monocrystals are required.

The aim of this work was to find the appropriate conditions for the growth of $BaSn_2Fe_4O_{11}$ crystals from the Fe_2O_3–SnO_2–BaO system in a $BaCl_2 \cdot B_2O_3$ flux environment using the high-temperature solution growth technique (HST), as well as to study its properties.

Experimental

The high-temperature solution method was used for the preparation of $BaSn_2Fe_4O_{11}$ single crystals and the "quasi"-ternary system SnO_2–BaO–Fe_2O_3 in a flux environment of $BaCl_2 \cdot B_2O_3$ was investigated. In all experiments, the amount of flux was kept constant during crystal growth. Samples were melted in platinum crucibles of 10- or 20-ml capacity. The soaking time and cooling rate were 2 hr and 15°C/hr, respectively, for all experiments.

0022-4596/89 $3.00

The matrix containing crystals was disintegrated with dilute HNO_3. The crystals were magnetic and could be separated from the disintegrated matrix using a permanent magnet. The composition of the crystals was determined chemically and with a microanalyzer. The nature of the crystals was checked by comparison of their X-ray diffraction pattern with published data.

The crystals were analyzed by powder and single-crystal X-ray diffraction. Intensity data were collected with graphite monochromated Mo$K\alpha$ radiation on a Nicolet P3/F diffractometer using the ω-2θ scan with a variable scan rate. Unit cell parameters were determined by the least-squares refinement of 25 reflections with Bragg angle between 20 and 50°. After averaging 1832 intensity measurements, 311 unique structure factors were obtained. The data collection summary is in Table IV.

The absorbers for Mössbauer measurements were prepared by powdering single crystals. The source was ^{57}Co in Rh and the spectra were measured with a 512-channel analyzer (Promeda), operated in the time mode and using Elscint constant-acceleration equipment. The velocity scale was calibrated with metallic iron which was also used as a reference for the isomer shift parameter. The spectra were analyzed by a nonlinear least-squares program assuming Lorentzian line shapes. By using thin absorbers (10 mg Fe/cm^2) and fine powdered samples, correction for the saturation and texture effects was not necessary.

Results and Discussion

In order to obtain the optimal flux composition which would be most effective for the growth of $BaSn_2Fe_4O_{11}$ crystals, the ternary system Fe_2O_3–SnO_2–BaO in a flux environment of the composition $BaCl_2 \cdot B_2O_3$ was investigated. The amount of flux was kept constant at 80 wt%. The $BaCl_2$ was selected due to the common ion with the phase grown from the flux, while B_2O_3 was added in order to decrease the viscosity of the flux.

During studies of this system, three main parameters were varied: the composition of the mixture at constant amount of flux, the cooling rate during grain growth, and the soaking temperature. Melting points of compositions were determined using DTA. It was established that the melting point of the composition studied was close to the melting point of $BaCl_2$: 980°C. First a temperature around 1100°C was selected and the system was investigated. The selected compositions were melted, heated for 2 hr at 1100°C, and cooled at 0.5°C/min to 800°C. The solidified content of the Pt crucible was then inspected visually and later disintegrated with dilute HNO_3 acid.

Five compositions were preliminarily tested. It was found that in the central region of the system (33 mole% BaO) a glass-forming region exists, while in the other parts of the system mainly magnetoplumbite phase was detected. By trial and error it was established that at higher soaking temperatures (T = 1200°C), in some parts of the system, a magnetic phase different from hexaferrite grows from the flux.

On the basis of preliminary investigations, two temperatures of 1300 and 1350°C were selected and crystal growth regions determined. The procedure was the same as in the preliminary test, except that in some cases the cooling rate was changed as stated elsewhere.

At 1300°C two phases were found to grow from the flux depending on its composition. In the BaO-rich part of the system, labeled as I in Fig. 1, small hexagonal magnetic platelets of a dark brown color were obtained. The X-ray diffraction pattern of these crystals was identical with that of $BaSn_2Fe_4O_{11}$ (*2*), and the composition was confirmed by microprobe analysis. In the Fe_2O_3-rich part of the system, labeled as II in Fig. 1, black, very magnetic hexagonal

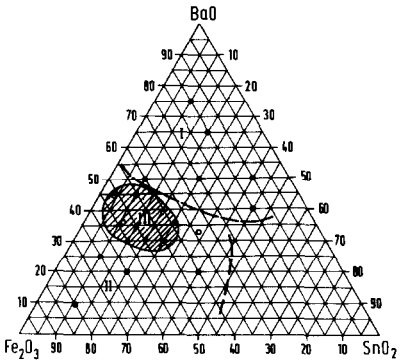

FIG. 1. The composition diagram BaO–SnO_2–Fe_2O_3 with crystal growth regions I, II, and III. The composition of the flux used was $BaCl_2 \cdot B_2O_3$.

platelets of $BaFe_{12}O_{19}$ were found to grow from the melt.

Thus, the system investigated at 1300°C can be divided in two crystal growth regions depending on the type of crystals grown from them; the BaO-rich part of the system where $BaSn_2Fe_4O_{11}$ crystals grow and the Fe_2O_3-rich part of the system where $BaFe_{12}O_{19}$ crystals grow. However, when the amount of Fe_2O_3 in the nominal composition exceeds about 70 mole% of Fe_2O_3, α-Fe_2O_3 can also be detected. Between the two growth regions a glass forming region was established, labeled as III (Fig. 1).

When a higher cooling rate was applied (>2°/min) during crystal growth at 1300°C from the BaO-rich part of the system, the crystals obtained were more magnetic. The X-ray diffraction pattern of these crystals show diffraction lines of both $BaSn_2Fe_4O_{11}$ and $BaFe_{12}O_{19}$. By examining crystals with an optical microscope (see Fig. 2) it was found that small black crystals of $BaFe_{12}O_{19}$ grow epitaxially on dark brown crystals of $BaSn_2Fe_4O_{11}$. In some cases during grain growth the furnace was switched off immediately after the soaking time and the Pt crucible with the melt was cooled in the critical temperature region between 1300 and 800°C at a cooling rate of approximately 600°C/hr. In this case predominately $BaFe_{12}O_{19}$ crystals were obtained. Thus, the cooling rate has a remarkable influence on the composition of the crystals grown. The cooling rate has a similar effect on the composition of the crystals grown as the composition of the flux itself. A higher amount of BaO in the flux and a lower cooling rate promote the growth of $BaSn_2Fe_4O_{11}$ crystals.

In the second course of experiments, the soaking temperature was raised above 1300°C. However, in this case at 1350°C the flux began to creep out of the crucible, and the evaporation became more pronounced. Particularly in the Fe_2O_3-rich part of the system, the whole flux creeped out of the crucible and/or evaporated (and the growth of crystals was impossible). However, in the BaO-rich part of the system the flux did not creep out of the crucible and the evaporation of the flux was accompanied by the growth of relatively large red-brown hexagonal platelets and red needles. The X-ray diffraction pattern of the hexagonal crystals was identical to that of $BaSn_2Fe_4O_{11}$, as was the composition. At the limit of resolution

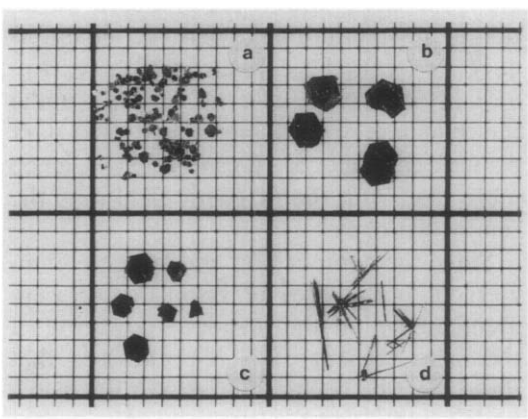

FIG. 2. Crystals from the various growth regions. (b) Large hexagonal platelets of $BaFe_{12}O_{19}$ grown from region II, (a) small hexagonal platelets of dark brown color, (c) larger hexagonal platelets of red-brown color of $BaSn_2Fe_4O_{11}$ composition grown from region I, and (d) red-brown needles of hollandite also grown from region I.

of chemical analysis, as well as microanalysis using the microanalyzer, no difference in the composition could be detected between the dark brown and red-brown hexagonal crystals. The red needles were identified as hollandite crystals, $Ba_xSn_{4-2x}Fe_{2x}O_8$, with lattice parameters a = 10.524 (3), b = 3.130 (1), c = 10.123 (3), and ζ = 91.25 (3).

Fig. 1 shows the compositions of the melt from which the crystals were grown and the appropriate crystal growth regions. I, BaO-rich part of the diagram from which $BaSn_2Fe_4O_{11}$ and hollandite crystals were grown; II, Fe_2O_3-rich part of the diagram where $BaFe_{12}O_{19}$ crystals grow; and III, glass-forming region.

A part of the investigation was focused on establishing the difference between the two types of $BaSn_2Fe_4O_{11}$ crystals. The red-brown crystals were, however, thinner so that some of the crystals were transparent. The powder was also of a different color: pale brown for the red-brown crystals, while the darker crystals gave a dark brown powder.

The crystal parameters of both crystals were the same within the standard deviation of the measurement. The second difference between the crystals, which was invariably observed, was the behavior under the influence of a magnetic field. The dark brown crystals of $BaSn_2Fe_4O_{11}$ aligned more readily in the magnetic field than the red-brown ones.

Since the composition and lattice parameters of both types of $BaSn_2Fe_4O_{11}$ were identical within the standard deviation of the measurement, it is hypothesized that there must be some difference in the distribution of Sn and Fe ions over appropriate lattice sites.

Structure Determination

Both types of $BaSn_2Fe_4O_{11}$ crystals were examined to ensure that they were suitable for structural analysis. In many cases, the dark brown crystals were found to be twinned, but some were suitable for structural refinement. The refinement of the red-brown crystals is in progress and will be reported elsewhere. Here we report the structural refinement of the dark brown crystals of $BaSn_2Fe_4O_{11}$.

During the first stage of the crystal structure refinement, the atomic positions within the $P6_3/mmc$ space group used by Haberey and Velicescu (*1*) were taken. The crystal data are given in Table I. The refinement by full-matrix least-squares included anisotropic temperature factors for all atoms. The 2d position was assumed to be pure Fe. Refinement was carried out by distributing the remaining Fe and Sn content among the 4e and 6g positions. Further, an occupancy factor of 1/2 at the 4f position was used in-

TABLE I

CRYSTAL DATA FOR $BaSn_2Fe_4O_{11}$

a =	5.969(2) Å
c =	13.764(3) Å
v =	424.6(4) Å^3
D_o =	6.12 g/cm^3
D_c =	6.05 g/cm^3
Z =	2
Space group $P6_3/mmc$	

TABLE II

FRACTIONAL COORDINATES AND OCCUPANCY FACTORS FOR $BaSn_2Fe_4O_{11}$

Atom	Position	x/a	y/b	z/c	Occup. factors (%)
Ba	2a	1/3	2/3	1/4	100
Fe(1)	4f	1/3	2/3	0.7287(3)	50
Fe(2)	4e	0	0	0.1433(9)	30
Sn(2)					70
Fe(3)	6g	1/2	0	0	76
Sn(3)					24
O (1)	6h	−0.1508(7)	−0.3017	1/4	100
O (2)	4f	1/3	2/3	−0.0814(7)	100
O (3)	12k	0.1763(6)	0.3526	0.0803(4)	100

stead of full occupancy of the 2d position as for $BaFe_{12}O_{19}$ (*3*). After this step *R* dropped to the ultimate value of 0.034. The fractional coordinates and lengths and angles for $BaSn_2Fe_4O_{11}$ are given in Tables II and III, respectively.

The compound is isostructural with $BaTi_2Fe_4O_{11}$ (*1*) and is related to that of the R block in $BaFe_{12}O_{19}$ (*3*). The structure consists of a hexagonal close-packed arrangement of oxygen atoms with some oxygens substituted by Ba. The Fe and Sn are located on octahedral and tetrahedral interstices. This means the structure is composed of BaO_3 layers in the mirror plane followed by two O_4 layers. The 4e and 6g octahedral lattice sites are statistically distributed by Sn and Fe. However, the occupation rate of Sn is noticeably higher at the 4e lattice sites than at the 6g lattice sites, as may be seen from Table II.

Looking at the structure of $BaSn_2Fe_4O_{11}$ one can see that two 4e octahedra share one common face located inside the mirror-plane, while sharing only corners with three 6g octahedra sites on the other side (Fig. 3).

This allows two adjacent 4e sites to be occupied by highly charged Sn^{4+} cations, as they can easily shift away from the common face toward the opposite unoccupied neighboring octahedra. With 70% of 4e sites occupied by Sn^{4+} cations one can expect a rather large proportion of such Sn^{4+}–Sn^{4+} neighboring pairs. As a matter of fact the tree $(Sn_2Fe_2)O_1$ distances are somewhat longer than the $(Sn_2Fe_2)O_3$ distances (Table III).

On the contrary, 6g octahedra sites share four edges with four other 6g octahedra sites building very rigid hexagonal Kagomé-like octahedra sheets. The distances between two neighboring octahedra inside such a sheet are too short to allow an occu-

TABLE III

INTERATOMIC DISTANCES (Å) AND ANGLES (°) OF $BaSn_2Fe_4O_{11}$

Distances (Å)		Angles (°)	
BaO_1	2.989(1) × 12	O_1BaO_1	68.0(0)
BaO_3	2.844(5) × 6	O_1BaO_1	113.5(0)
		O_1BaO_3	118.5(1)
			91.8(1)
			59.4(1)
			61.4(1)
		O_3BaO_3	146.8(1)
			110.4(3)
			59.2(2)
	Fe^{3+} bipyramid		
Fe_1O_1	1.909(8) × 3		
		$O_1Fe_1O_1$	117.7(3)
Fe_1O_2	2.028(11) × 1		
	2.613(11) × 1	$O_2Fe_1O_2$	98.8(1)
	Fe^{3+}, Sn^{4+} octahedron		
$(Fe_2Sn_2O_1$	2.142(6) × 3		
		$O_1Fe_2O_1$	78.2(2)
$(Fe_2Sn_2)O_3$	2.018(7) × 3		
		$O_1Fe_2O_3$	88.0(2)
			162.1(2)
		$O_3Fe_2O_3$	102.9(2)
$(Fe_3Sn_3)O_3$	2.007(2) × 3		
		$O_3Fe_3O_3$	88.9(2)
$(Fe_3Sn_3)O_2$	2.055(5) × 3		91.1(2)
		$O_3Fe_3O_2$	94.6(2)
			85.4(2)

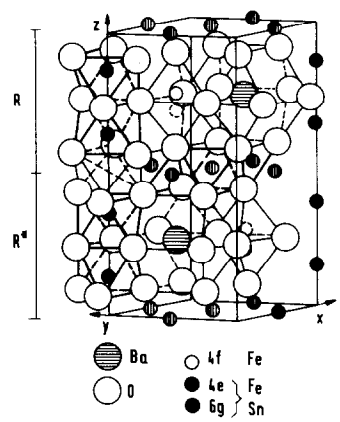

FIG. 3. Unit cell of the structure of $BaSn_2Fe_4O_{11}$: shaded large circles, Ba; open circles, O; small open circles, Fe (4f); small shaded circles, Fe, Sn (6g); and small solid circles, Fe, Sn (4e).

TABLE IV

DATA COLLECTION SUMMARY

Temperature (K)	293(1)
Diffractometer	Nicolet P3/F
Scan method	w/2θ
2θ scan width (°C)	4–79°
Radiation	Mo$K\alpha$ (0.71069 Å)
Size of crystal (mm)	2
Linear absorption	No correction
Coefficient (cm^{-1})	173.5
Measured reflections	1832
Averaged reflections	311 (list of structure factors)

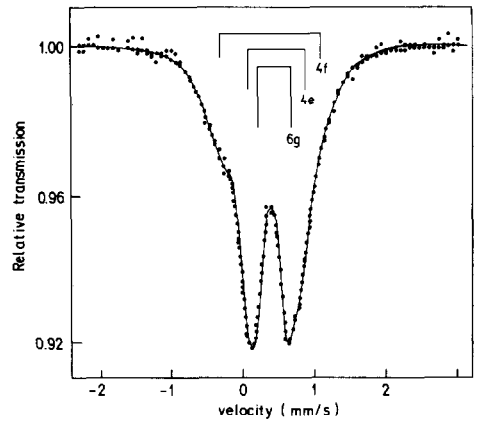

FIG. 4. Mössbauer spectrum of ^{57}Fe in dark brown powdered crystals of $BaSn_2Fe_4O_{11}$ at room temperature taken with the source $^{57}Co/Rh$.

pancy with so many (up to five) adjacent tetravalent Sn^{4+} cations. So these sites are likely to be occupied by a majority of trivalent cations as can be observed from the occupancy factor of these sites. With 24% Sn^{4+} on the 6g sites one can expect each Sn^{4+} to be surrounded by three Fe^{3+} and one Sn^{4+} octahedra, which seems quite reasonable.

Mössbauer Spectroscopy

Mössbauer spectra measured in the paramagnetic state from 77 to 860 K are essentially similar for the dark and red-brown-type samples. They display the superposition of three doublet subspectra due to quadrupole interaction between the nuclear quadrupole moment of the iron nucleus and the electric field gradient (efg) tensors at 4e, 6g, and 4f iron sites in the hexagonal R structure (rombohedral structure). Typical spectrum of ^{57}Fe in $BaSn_2Fe_4O_{11}$ at room temperature is shown in Fig. 4.

Measured spectra were satisfactorily fitted by assuming three overlapped doublets with Lorentzian line shape. Some constraints regarding the widths and the intensities of resonance lines were applied during the fitting procedure. The best fit to the data was obtained for the hyperfine parameters of the dark brown and red-brown samples given in Table V. The subspectrum of the quasi-tetrahedral 4f site for each sample has been unambiguously identified due to a very large efg tensor caused by the strong deviation from cubic symmetry.

The isomer shift and quadrupole splitting parameters of octahedral 6g, 4e, and quasi-tetrahedral 4f subspectra are similar to previous results (*4*) representing Fe^{3+} ions in a high-spin $3d^5$ configuration. The relatively high value of the quadrupole splitting parameter for the quasi-tetrahedral doublet is an exception, but it can also be ascribed to Fe^{3+} ions on the basis of the isomer shift parameter and its temperature dependence.

TABLE V

HYPERFINE PARAMETERS OF ^{57}Fe IN $BaFe_4Sn_2O_{11}$ AT 295 K

Site	IS (mm/sec)		QS (mm/sec)		Γ (mm/sec)		Area (%)	
	a	b	a	b	a	b	a	b
6g	0.35	0.35	0.44	0.43	0.28	0.36	47	55
4e	0.34	0.34	0.75	0.75	0.31	0.35	31	28
4f	0.23	0.24	1.38	1.38	0.40	0.34	22	17

Note. a, Dark brown; b, red brown; IS, isomer shift relative to metallic iron ±0.02; QS, quadrupole splitting, ±0.01; Γ, full width at half maximum ±0.01; area, relative areas of quadrupole doublets ±2%.

Some broadening of the resonance lines of various subspectra could be direct evidence for several configurations due to distribution of iron and tin ions over the two octahedral sites identified also by the X-ray diffraction data.

Assuming a similar recoil-free fraction for all iron ions, the occupation rate of various cation sites in R structure of $BaSn_2Fe_4O_{11}$ can be related to the relative areas of quadrupole split doublets given in Table V. However, in comparison to X-ray diffraction data (Table II) Mössbauer doublet area results predict a reduced occupation rate for quasi-tetrahedral (4f) sites and strong preference for the octahedral 4e sites either for dark or red-brown crystals. But, anyhow, relative areas are still consistent with the previously reported results (*4*) indicating strong dependence of cation distribution on the crystal growth procedure. Since we have eliminated the saturation and texture effects on the areas and intensity asymetries of Mössbauer resonance lines, it seems reasonable to suppose that the main reason for the slight deviation in occupation rates obtained by X-ray and Mössbauer analysis might be ascribed to the uncritical assumption that all iron ions in R structure exhibit a similar recoil-free factor. A reduced recoil-free fraction for iron ions at quasi-tetrahedral 4f sites relative to the octahedral ones can be expected in the measured temperature region due to the diffusional motion of iron ions between two equivalent sites, as shown for bipyramidal 2d sites in the M structure of $BaFe_{12}O_{19}$ ferrites (*3, 5*).

Conclusions

The growth of $BaSn_2Fe_4O_{11}$ crystals from a $BaCl_2 \cdot B_2O_3$ flux depends on the soaking temperature, the composition of flux, and the cooling rate.

Sn and Fe are distributed over 4e and 6g lattice sites. Due to electrostatic and steric reasons, the 4e lattice sites are more suitable for the accomodation of high-valent larger Sn atoms.

The hyperfine parameters of ^{57}Fe indicate that the iron local and electronic structures for dark and red-brown crystals are quite similar. The difference between both types of crystals found in the relative areas of quadrupole doublet subspectra indicate that the occupation of lattice sites depends on the crystal growth conditions.

There are some deviations in the results for occupation of iron sites obtained by Mössbauer spectra and by X-ray diffraction data. The difference is probably due to the fact that equal recoil-free fraction was assumed for all iron lattice sites.

On the basis of the current investigation no quantitative difference between dark brown and red-brown $BaSn_2Fe_4O_{11}$ crystals could be found. The true difference between both types of crystals is most probably limited to the cation distribution between different lattice sites and a relatively small difference in the chemical composition of crystals. In addition, contamination with SnO_2 was found (*4*) during the study of $BaSn_2Fe_4O_{11}$ crystals by Mössbauer spectroscopy of Sn nuclei.

References

1. F. Haberey and M. Velicescu, *Acta Crystallogr. B*, 1507 (1974).
2. M. C. Cadee and D. J. W. Ijdo, *J. Solid State Chem.* **52,** 302 (1984).
3. X. Obrados, A. Collomb, M. Pernet, D. Samaras, and J. C. Joubert, *J. Solid State Chem.* **56,** 171 (1985).
4. T. Birchall, C. Hallet, and D. Hanžel, *Solid State Commun.* **56,** 77 (1985).
5. E. Kreber, U. Gonser, and A. Trautwein, *J. Chem. Solids* **36,** 263 (1975).